Optimal Decentralized Protocols for Electric Vehicle Charging

Lingwen Gan Ufuk Topcu Steven Low

***Abstract*—We propose decentralized algorithms for optimally scheduling electric vehicle charging. The algorithms exploit the elasticity and controllability of electric vehicle related loads in order to fill the valleys in electric demand profiles. We formulate a global optimization problem whose objective is to impose a generalized notion of valley-filling, and study the properties of optimal charging profiles. We then give two decentralized algorithms, one synchronous (i.e., information update takes place in each iteration) and one asynchronous (i.e., EVs may use outdated information with bounded delay in some of the iterations) to solve the problem. In each iteration of the proposed algorithms, electric vehicles choose their own charging profiles according to the price profile broadcast by the utility, and the utility updates the price profile to guide their behavior. The algorithms are guaranteed to converge to optimal charging profiles (that are as "flat" as they can possibly be) irrespective of the specifications (e.g., maximum charging rate and deadline) of electric vehicles. Furthermore, they do not require any coordination among the electric vehicles, hence their implementation requires low communication and computation capability.**

***Index Terms*—Distributed optimal control; electrical vehicle charging; controllable electric loads.**

Notation

t	time index, $t \in \mathcal{T} := \{1, \ldots, T\}$
n	index of electric vehicles (EVs), $n \in \mathcal{N} := \{1, \ldots, N\}$
D	base demand profile
r_n	charging profile of EV n
r	charging profile of all EVs
R_r	aggregated charging profile corresponding to r
$\overline{r}_n$	charging rate upper bound for EV n
R_n	charging rate sum of EV n
$\mathcal{F}_n$	set of feasible charging profiles for EV n
$\mathcal{F}$	set of feasible charging profiles for all EVs
$\mathcal{O}$	set of optimal charging profiles
p	price profile
$\preceq$	if $a, b \in \mathbb{R}^n$, $a \preceq b \Leftrightarrow a_i \le b_i$ for all $i \in \{1, \ldots, n\}$
x^+	$\max\{0, x\}$
$\langle x, y \rangle$	for $x, y \in \mathbb{R}^n$, $\langle x, y \rangle := \sum_{k=1}^{n} x_k y_k$

I. Introduction

Electric vehicles (EVs) offer significant potential for increasing energy efficiency in transportation, reducing greenhouse gas emissions, and relieving reliance on foreign oil [1]. Currently, several types of EVs are either already in the U.S. market or about to enter [2], and electrification of transportation is at the forefront of many research and development agendas [3]. On the other hand, the potential comes with a multitude of challenges including those in the integration into the electric power grid. EV charging increases the electric loads, and potentially amplifies the peak demand or creates new peaks in electricity demand [4]. It also increases the demand side uncertainties, and presumably reduces the distribution circuit and transformer lifespan [5]. Moreover, power losses and voltage variations become more likely [6].

The simulation-based study in [7] suggests that, if no regulation on EV charging is implemented, even a 10% penetration of EVs may cause unacceptable variations in voltage profiles. On the other hand, many studies demonstrate that adopting "smart" charging strategies can mitigate some of the integration challenges, defer infrastructure investment needed otherwise, and even stabilize the grid. For example, scheduling EV charging so that aggregated EV load fills the overnight valley in demand may reduce daily cycling of power plants and operational costs of electricity utilities. Furthermore, the energy stored in EVs may be utilized as an alternative ancillary service resource [8] for regulating voltage profiles, ride-through support for fault protection, and even compensating fluctuating renewable energy generation [9].

Studies on EV charging control roughly fall into three categories: effect of time-of-use rates [10], coordinated charging scheduling [6], [9], [11], and decentralized scheduling [12] [13]. Reference [10] explores the effect of higher price during peak hours on shifting EV load, but does not provide strategies for setting the price. Reference [6], [9], [11] study centralized control strategies that minimize power losses and load variance, or maximize load factor and supportable EV penetration level. These strategies require a centralized structure to collect information from all the EVs and centrally optimize over their charging profiles. Reference [12] demonstrates, through a simulation-based study, that total demand profile can be flattened by introducing load-side participation into the power market. They propose a decentralized strategy, but do not provide any analytical optimality guarantees. Reference [13] proposes another decentralized charging strategy, and proves its optimality in the case where all EVs plug in at the same time with the same state-of-charge (SOC), and have the same deadline and allowable charging rates. For future reference, we call this setting *homogeneous*.

The contributions of the current paper include the following. First, we define optimal charging profiles of EVs explicitly (this definition generalizes the implicit definition in [13]). Second, we propose a decentralized charging strategy that guarantees optimality in both homogeneous and non-homogeneous cases, where EVs can plug-in at different times

The authors are with Engineering and Applied Sciences at the California Institute of Technology, e-mail: lgan@caltech.edu; utopcu@cds.caltech.edu; slow@caltech.edu.

with different SOC, have different maximum charging speed and deadlines. Third, we remove the artificial tracking error penalty in EV owners' objective in [13] by introducing another penalty term that vanishes at convergence. Hence, this penalty term does not affect the optimal charging profiles to be adopted by the EVs. Finally, we modify the decentralized algorithm to accommodate asynchronous computations, i.e., EVs may make their decisions at different times with potentially outdated information.

The rest of the paper is organized as follows. Section II formulates the EV charging protocol design problem as a finite-horizon optimal control problem. Section III explores properties of optimal charging profiles of this optimal control problem. Section IV is dedicated to the presentation of two decentralized optimization algorithms for solving the optimal control problem and their convergence proofs. Numerical case studies are presented in section V, and some of the limitations and potential extensions of the proposed work are summarized in section VI.

II. Problem Formulation

Consider a scenario where an electric utility negotiates with N electric vehicles (EVs) over T time slots of length ΔT on their charging profiles. The utility is assumed to know the inelastic base demand profile (aggregated non-EV demand) and aims to shape the aggregated charging profile of EVs to flatten the total demand (base demand plus EV demand) profile. Each EV can charge after it plugs in and needs to be fully charged by its deadline. In each time slot, its charging rate is constant. Let $D(t)$ denote the base load in slot t, $r_n(t)$ denote the charging rate of EV n in slot t, $r_n := (r_n(1), \ldots, r_n(T))$ denote the charging profile of EV n, for $n \in \mathcal{N} := \{1, \ldots, N\}$ and $t \in \mathcal{T} := \{1, \ldots, T\}$. The term "negotiate" will be clear in section IV where decentralized algorithms for solving the finite-horizon optimal control problem formulated in this section are presented. Roughly speaking, this optimal control problem formalizes the intent of flattening the total demand profile. To this end, consider the objective function

$$L(r) = L(r_1, \ldots, r_N) := \sum_{t=1}^{T} U\left(D(t) + \sum_{n=1}^{N} r_n(t)\right). \quad (1)$$

In (1) and hereafter, $r := (r_1, \ldots, r_N)$ denotes a charging (rate) profile. The map $U : \mathbb{R} \to \mathbb{R}$ is strictly convex. The charging rate $r_n(t)$, $t = 1, \ldots, T$ of EV n is considered to take values in the interval $[0, \overline{r}_n]$ for some given $\overline{r}_n \succeq 0$. In order to impose arrival time and deadline constraints, $\overline{r}_n$ is considered to be time-dependent with $\overline{r}_n(t) = 0$ for slots t before the arrival time and after the deadline of EV n. Hence

$$0 \le r_n(t) \le \overline{r}_n(t), \ n \in \mathcal{N}, \ t \in \mathcal{T}. \quad (2)$$

For EV $n \in \mathcal{N}$, let B_n, $s_n(0)$, and η_n denote its battery capacity, initial state of charge and charging efficiency. The constraint that EV n should be fully charged by its deadline is captured by the total energy stored over time horizon

$$\eta_n \sum_{t \in \mathcal{T}} r_n(t) \Delta T = B_n \left(1 - s_n(0)\right), \ n \in \mathcal{N}. \quad (3)$$

Define

$$R_n := B_n \left(1 - s_n(0)\right) / (\eta_n \Delta T)$$

for $n \in \mathcal{N}$, then (3) can be written as

$$\sum_{t=1}^{T} r_n(t) = R_n, \ n \in \mathcal{N}. \quad (4)$$

Reference [14] summarizes some of the recently announced EV models and typical values of $\overline{r}_n$ and R_n can be derived for these models (and used in the numerical case studies in section V).

Definition 1: Let $U : \mathbb{R} \to \mathbb{R}$ be strictly convex. A charging profile $r = (r_1, \ldots, r_N)$ is

1) *feasible*, if it satisfies the constraints (2) and (4);
2) *optimal*, if it solves

$$\begin{array}{ll} \underset{r_1,\ldots,r_N}{\text{minimize}} & L(r_1, \ldots, r_N) \\ \text{subject to} & 0 \preceq r_n \preceq \overline{r}_n, \ n \in \mathcal{N}, \\ & \sum_{t=1}^{T} r_n(t) = R_n, \ n \in \mathcal{N}; \end{array} \quad (5)$$

3) *valley-filling*, if there exists $A \in \mathbb{R}$ such that

$$\sum_{n \in \mathcal{N}} r_n(t) = \left[A - D(t)\right]^+, \ t \in \mathcal{T}.$$

Remark 1: Optimality of charging profile r is independent of the choice of U (Theorem 2). If r is optimal with respect to one strictly convex U, it is optimal with respect to any other strictly convex U. Therefore, we can choose $U(x) = x^2$ without loss of generality, and see that optimal charging profiles minimize the l_2 norm of the total demand profile. Since the l_1 norm is a constant for all feasible r due to (4), minimizing the l_2 norm "flattens" the total demand profile.

Remark 2: The map $p := U'$ can be interpreted as the price of electricity usage. Since U is strictly convex, p is high in slots t with high total demand. Hence, shifting electricity usage to other slots is favored.

III. Optimal Charging Profile

In this section, we investigate the properties of optimal charging profiles. For notational simplicity, for a given charging profile $r = (r_1, \ldots, r_N)$, let

$$R_r := \sum_{n \in \mathcal{N}} r_n$$

denote the aggregated charging profile corresponding to r.

Property 1: If a feasible charging profile r is valley-filling, then it is optimal.

Proof: Let r be feasible and valley-filling. Note that R_r is the unique solution to the problem

$$\begin{array}{ll} \underset{R}{\text{minimize}} & \sum_{t \in \mathcal{T}} U\left(D(t) + R(t)\right) \\ \text{subject to} & \sum_{t \in \mathcal{T}} R(t) = \sum_{n \in \mathcal{N}} R_n, \\ & R \succeq 0. \end{array} \quad (6)$$

For any feasible r', $R_{r'}$ is feasible for (6). Furthermore, the objective function in (6) evaluated at $R_{r'}$ is equal to $L(r')$. Hence, the optimal value d_* of (6) is a lower bound for the

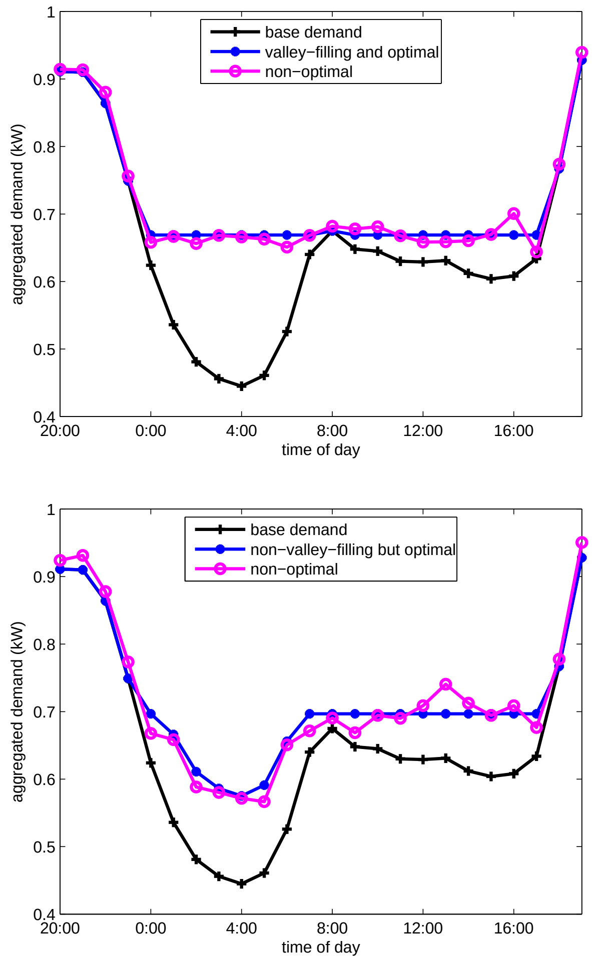

Fig. 1. Base demand profile is the average residential load in the service area of Southern California Edison (SCE) from 20:00 on February 13, 2011 to 19:00 on February 14, 2011 [15]. Optimal aggregated charging profile curve corresponds to the outcome of Algorithm A1 with $U(x) = x^2$. With different specifications for EVs (e.g., maximum charging rate $\overline{r}_n$), optimal charging profile can be valley-filling (top) or non-valley-filling (bottom). A hypothetical non-optimal curve is shown with the marker o.

optimal value p_* of (5). The aggregated profile R_r attains d_*, so $L(r) = d_* \leq p_*$. Since r is feasible, it is optimal. □

Let

$$\mathcal{F}_n := \left\{ r_n \middle| \ 0 \preceq r_n \preceq \overline{r}_n, \sum_{t\in\mathcal{T}} r_n(t) = R_n \right\}$$

denote the set of feasible charging profiles for EV n. Then,

$$\mathcal{F} := \mathcal{F}_1 \times \cdots \times \mathcal{F}_N$$

is the set of feasible charging profiles $r = (r_1, \ldots, r_N)$.

Property 2: If $\mathcal{F}$ is non-empty, optimal charging profiles exist.

Proof: Since $\mathcal{F}_n$ is compact, $\mathcal{F}$ is also compact. Since L is continuous, its minimum value is attained at some $r \in \mathcal{F}$, which is an optimal charging profile. □

Valley-filling is our intuitive notion of optimality. However, it may not be always achievable. For example, the "valley" in inelastic demand may be so deep that even if all EVs charge at their maximum rate, it is still not completely filled, e.g., at 4:00 in Figure 1 (bottom). Besides, EVs may have stringent deadline constraints such that the potential for shifting the load over time to yield valley-filling is limited. Our constructive definition of optimality relaxes these restrictions as a result of Property 2. Moreover, it agrees with the intuitive notion of optimality when valley-filling is achievable as a result of Property 1, illustrated in Figure 1 (top). We now establish an equivalence relation between charging profiles, and show that optimal charging profiles form an equivalence class.

Definition 2: Feasible charging profiles r and r' are *equivalent*, denoted by $r \sim r'$, provided that $R_r = R_{r'}$, i.e., r and r' have the same aggregated charging profile.

It is easy to check that the relation $\sim$ is an equivalence relation. Define equivalence classes $\{r' \in \mathcal{F} | \ r' \sim r\}$ with representatives $r \in \mathcal{F}$, and

$$\mathcal{O} := \{r \in \mathcal{F} \mid r \text{ optimal}\}$$

as the set of optimal charging profiles.

Theorem 1: If $\mathcal{F}$ is non-empty, then $\mathcal{O}$ is non-empty, compact, convex, and an equivalence class of the relation $\sim$.

Proof: Property 2 implies that $\mathcal{O}$ is nonempty. Let r be a charging profile in $\mathcal{O}$, and define equivalence class

$$\mathcal{O}' := \{r' \in \mathcal{F} \mid r' \sim r\}.$$

Then $\mathcal{O}'$ is closed and convex. Since $\mathcal{F}$ is compact, the set $\mathcal{O}'$, as a closed subset of $\mathcal{F}$, is also compact. Hence, $\mathcal{O}'$ is non-empty, compact, convex, and an equivalence class.

We only need to prove that $\mathcal{O} = \mathcal{O}'$. It is easy to see that $\mathcal{O}' \subseteq \mathcal{O}$, and we prove $\mathcal{O} \subseteq \mathcal{O}'$ as following. For any $r' \in \mathcal{O}$, from the first order optimality condition for (5),

$$\langle U'(D + R_r), R_{r'} - R_r \rangle = 0,$$
$$\langle U'(D + R_{r'}), R_r - R_{r'} \rangle = 0.$$

Hence,

$$\langle U'(D + R_r) - U'(D + R_{r'}), R_r - R_{r'} \rangle = 0,$$

$R_r = R_{r'}$, $r' \sim r$, $r' \in \mathcal{O}'$, and $\mathcal{O} \subseteq \mathcal{O}'$. □

Corollary 1: Optimal charging profile may not be unique.

Theorem 2: The set $\mathcal{O}$ of optimal charging profiles does not depend on the choice of U. That is, if r^* is optimal with respect to one strictly convex U, then r^* is also optimal with respect to any other strictly convex $\tilde{U}$.

Proof: Let $\hat{\mathcal{O}}$ denote the set of optimal charging profiles with respect to $\hat{U}(x) = x^2$, $\mathcal{O}_U$ denote the set of optimal charging profiles with respect to an arbitrary, strictly convex U. We only need to show that $\mathcal{O}_U = \hat{\mathcal{O}}$. According to Theorem 1, $\mathcal{O}_U$ is an equivalence class represented by some charging profile $r^* = (r_1^*, \ldots, r_N^*)$. Define $R^* := R_{r^*}$, then from the optimality of r^* with respect to U,

$$\langle U'(D + R^*), r_n' - r_n^* \rangle \geq 0$$

for $n \in \mathcal{N}$ and $r_n' \in \mathcal{F}_n$. Hence, r_n^* minimizes $\langle U'(D + R^*), r_n \rangle$ over $r_n \in \mathcal{F}_n$. Since U' is strictly increasing and $\sum_{t=1}^{T} r_n(t)$ is a constant for $r_n \in \mathcal{F}_n$, r_n^* minimizes $\langle D + R^*, r_n \rangle$ over $r_n \in \mathcal{F}_n$, hence

$$\langle D + R^*, r_n' - r_n^* \rangle \geq 0$$

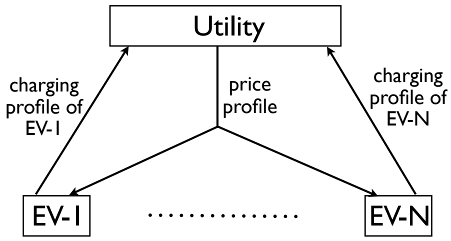

Fig. 2. Schematic view of the information flow patterns between the utility and the EVs in Algorithm A1. Given the (predicted) price profile, the EVs choose their charging profiles independently. The utility guides their decisions by altering the electricity price profile based on total demand profile.

for $n \in \mathcal{N}$ and $r'_n \in \mathcal{F}_n$. Sum up over $n \in \mathcal{N}$ to obtain

$$\langle D + R_r, R_{r'} - R_r \rangle \geq 0$$

for all $r' \in \mathcal{F}$, which is the first order optimality condition for minimizing $L(r)$ with $U(x) = x^2$. Hence, $r^* \in \hat{\mathcal{O}}$, and it follows from Theorem 1 that $\mathcal{O}_U = \hat{\mathcal{O}}$. □

The optimal solution to (5) provides a uniform means for defining optimality even when valley-filling is not achievable, and Theorem 2 implies that this optimality notion is intrinsic, independent of the choice of U.

IV. Decentralized Algorithms

In this section, we propose two decentralized algorithms, Algorithms A1 and A2 discussed below, for computing optimal charging profiles as the solution of the finite-horizon optimal control problem in (5). By decentralized, we mean that EVs choose their own charging profiles, instead of being instructed by a centralized infrastructure. The utility only uses control signals, e.g. prices, to guide EVs' decisions. We assume that all EVs are available for negotiation at the beginning of the planning horizon (even though they do not necessarily charge as reflected by time-varying $\overline{r}_n$). Algorithm A1 is a synchronous algorithm requiring all EVs to make decisions at the same time with up-to-date information, while Algorithm A2 is asynchronous, allowing EVs to make decisions at different times using potentially outdated information with bounded delays in information update. In the end, we prove the convergence of both algorithms to optimal charging profiles under certain mild conditions.

A. Synchronous Decentralized Algorithm

We now present the basic decentralized offline algorithm and prove its convergence to optimal charging profiles. Figure 2 shows the information exchange between the utility and the EVs for the implementation of this algorithm. Given the electricity price profile broadcast by the utility, each EV chooses its charging profile independently, and reports back to the utility. The utility guides their behavior by altering the electricity price profile. We assume U' is Lipschitz with the Lipschitz constant $\beta > 0$, i.e.,

$$|U'(x) - U'(y)| \leq \beta |x - y|$$

for all x, y.

Algorithm A1: Given planning horizon $\mathcal{T}$, maximum number of iterations $K \in \mathbb{N}$, error tolerance $\epsilon > 0$, base load profile D, the number of EVs N, charging capacity R_n and charging rate upper bound $\overline{r}_n$ for EV $n \in \mathcal{N}$, pick a step size γ satisfying

$$0 < \gamma < \frac{1}{N\beta}.$$

1) Initialize the price profile and the charging profile as
$$p^0(t) := U'(D(t)), \; r_n^0(t) := 0$$
for $t \in \mathcal{T}$ and $n \in \mathcal{N}$, $k \leftarrow 0$.
2) The utility broadcasts the current price profile p^k and the step size γ.
3) Each EV $n \in \mathcal{N}$ calculates a new charging profile
$$r_n^{k+1} := \underset{r_n \in \mathcal{F}_n}{\text{argmin}} \sum_{t \in \mathcal{T}} p^k(t) r_n(t) + \frac{1}{2\gamma} \left(r_n(t) - r_n^k(t) \right)^2. \tag{7}$$
4) The utility collects charging profiles r_n^{k+1} from all EVs $n \in \mathcal{N}$, and updates the price as
$$p^{k+1}(t) := U' \left(D(t) + \sum_{n=1}^{N} r_n^{k+1}(t) \right) \tag{8}$$
for $t \in \mathcal{T}$.
If $\left\| p^{k+1} - p^k \right\|_2 \leq \epsilon$, return $p^{k+1}, \; r_n^{k+1}$ for all n.
5) If $k < K$, $k \leftarrow k + 1$, and go to step (2).
Else, return $p^K, \; r_n^K$ for all n.

Remark 3: The two terms in in the summation in (7) are in different units; therefore, certain scaling factors are needed to be strictly formal. These scaling factors are omitted for notational brevity.

Remark 4: The step size γ can be combined in price in each iteration. By changing p^k to γp^k and γ to 1, the utility only needs to broadcast price profile p^k in step (2).

Remark 5: Algorithm A1 can be decentralized, since the utility does not need to know R_n and $\overline{r}_n$, and EVs do not need to know D and N.

In each iteration, the algorithm can be split into two parts. In the first part, EV n updates its charging profile to minimize its objective function as (7). There are two terms in the objective: the first term is the electricity cost and the second term penalizes deviations from the profile computed in the previous iteration. The extra penalty term ensures convergence of Algorithm A1, and vanishes as $k \to \infty$ (see Theorem 4). Hence, the objective function of each EV boils down to its electricity cost as $k \to \infty$. In the second part of the iteration, the utility updates the price profile according to (8). It sets higher prices for slots with higher total demand, to give EVs the incentive to shift their charging rates to slots with lower total demand in the next iteration. As a result, the total demand may be flattened as iteration goes on.

We now establish the convergence of Algorithm A1 to the set $\mathcal{O}$ of optimal charging profiles. Let the superscript k for each variable denote its respective value in iteration k. For example, r_n^k denotes the charging profile of EV n in iteration k. Similarly,

$$R^k := \sum_{n=1}^{N} r_n^k$$

denotes the aggregated charging profile in iteration k.

Lemma 1: If the set $\mathcal{F}$ of feasible charging profiles is non-empty, then the inequality

$$\langle \gamma p^k, r_n^{k+1} - r_n^k \rangle \le - \left\| r_n^{k+1} - r_n^k \right\|_2^2 \quad (9)$$

holds for $n \in \mathcal{N}$ and $k \ge 1$. The equality in (9) is attained if and only if $r_n^{k+1} = r_n^k$.

Proof: For $n \in \mathcal{N}$ and $k \ge 1$, from the first order optimality condition for (7), it follows that

$$\langle \gamma p^k + r_n^{k+1} - r_n^k, r_n - r_n^{k+1} \rangle \ge 0 \quad (10)$$

for all $r_n \in \mathcal{F}_n$. Since $r_n^k \in \mathcal{F}_n$,

$$\langle \gamma p^k + r_n^{k+1} - r_n^k, r_n^k - r_n^{k+1} \rangle \ge 0,$$

and (9) follows. □

Lemma 2: If $\mathcal{F}$ is non-empty, then for $n \in \mathcal{N}$ and $k \ge 1$, $r_n^{k+1} = r_n^k$ if and only if

$$\langle p^k, r_n - r_n^k \rangle \ge 0 \quad (11)$$

for all $r_n \in \mathcal{F}_n$.

Lemma 2 follows from (10) and strict convexity of (7).

Theorem 3: If $\mathcal{F}$ is non-empty, then $r^k \to \mathcal{O}$ as $k \to \infty$.

Proof: Define $D^k := D + R^k$, then

$$\begin{aligned}
L(r^{k+1}) &= \sum_{t=1}^{T} U\left(D^{k+1}(t)\right) \\
&\le \sum_{t=1}^{T} U\left(D^k(t)\right) - p^{k+1}(t)\left(R^k(t) - R^{k+1}(t)\right) \\
&= L(r^k) + \langle p^{k+1}, R^{k+1} - R^k \rangle \\
&\le L(r^k) + \langle p^k + \beta\left(R^{k+1} - R^k\right), R^{k+1} - R^k \rangle \\
&= L(r^k) + \beta \left\| R^{k+1} - R^k \right\|_2^2 + \sum_{n=1}^{N} \langle p^k, r_n^{k+1} - r_n^k \rangle \\
&\le L(r^k) + \beta \left\| R^{k+1} - R^k \right\|_2^2 - \frac{1}{\gamma} \sum_{n=1}^{N} \left\| r_n^{k+1} - r_n^k \right\|_2^2 \\
&\le L(r^k) + \left(N\beta - \frac{1}{\gamma} \right) \sum_{n=1}^{N} \left\| r_n^{k+1} - r_n^k \right\|_2^2 \quad (12) \\
&\le L(r^k)
\end{aligned}$$

for $k \ge 1$. The first inequality is due to convexity of U, the second inequality is due to the definition of β, the third inequality is due to Lemma 1, and the fourth inequality is due to the Cauchy-Schwarz theorem. It is easy to check that $L(r^{k+1}) = L(r^k)$ if and only if $r^{k+1} = r^k$.

If $r^{k+1} = r^k$, then it follows from Lemma 2 that

$$\langle p^k, r_n' - r_n^k \rangle \ge 0$$

for all n and $r_n' \in \mathcal{F}_n$. Hence,

$$\langle p^k, R_{r'} - R^k \rangle = \sum_{n=1}^{N} \langle p^k, r_n' - r_n^k \rangle \ge 0 \quad (13)$$

for all $r' = (r_1', \ldots, r_N') \in \mathcal{F}$, which is the first order optimality condition for solving(5). It follows that $r^k \in \mathcal{O}$. On the other hand, if $r^k \in \mathcal{O}$, then $L(r^k) \le L(r^{k+1}) \le L(r^k)$. Hence,

$$L(r^{k+1}) = L(r^k) \Leftrightarrow r^{k+1} = r^k \Leftrightarrow r^k \in \mathcal{O}.$$

Finally, the facts that $\mathcal{F}$ is compact, every $r \in \mathcal{O}$ minimizes L, and $L(r^{k+1}) < L(r^k)$ if $r^k \notin \mathcal{O}$ imply that $r^k \to \mathcal{O}$ as $k \to \infty$. □

Corollary 2: A charging profile r is stationary for Algorithm A1, i.e., if $r^{\bar{k}} = r$ for some $\bar{k} \ge 0$ then $r^k = r$ for all $k \ge \bar{k}$, if and only if $r \in \mathcal{O}$.

The proof of Corollary 2 follows from the fact that $r^{k+1} = r^k$ if and only if $r^k \in \mathcal{O}$.

Theorem 4: Let r^* be an optimal charging profile. If $\mathcal{F}$ is non-empty, then

- the aggregated charging profile converges to that of r^*, i.e.,
$$\lim_{k \to \infty} R^k = R_{r^*};$$
- the price profile converges to that of r^*, i.e.,
$$\lim_{k \to \infty} p^k = U'(D + R_{r^*});$$
- the difference between two consecutive charging profiles of each EV converges to 0, i.e.,
$$\lim_{k \to \infty} \left\| r_n^{k+1} - r_n^k \right\|_2 = 0$$
for all $n \in \mathcal{N}$.

Proof: Theorem 3 implies that we can find a sequence $\{r^{*k}\}_{k \ge 1} \in \mathcal{O}$, such that $\|r^k - r^{*k}\| \to 0$ as $k \to \infty$. Since $\mathcal{O}$ is an equivalence class of $\sim$, $R_{r^{*k}} = R_{r^*}$. Hence $R^k \to R_{r^*}$ as $k \to \infty$. The price profile converges due to (8). Furthermore, the inequality in (12) implies that

$$L(r^k) - L(r^{k+1}) \ge \left(\frac{1}{\gamma} - N\beta \right) \sum_{n=1}^{N} \left\| r_n^{k+1} - r_n^k \right\|_2^2$$

for $k \ge 1$. Since $L(r^k) - L(r^{k+1}) \to 0$ as $k \to \infty$, it follows that for all $n \in \mathcal{N}$, $||r_n^{k+1} - r_n^k||_2 \to 0$ as $k \to \infty$. □

Theorem 3 shows the convergence of r^k to the optimal set $\mathcal{O}$ while Theorem 4 focuses on the convergence of R^k and p^k to the optimal value R_{r^*} and $U'(D + R_{r^*})$. Since the change in the charging profile for EV n between consecutive iterations vanishes as $k \to \infty$, the objective function (7) approximates the electricity cost after a certain number of iterations. It follows from (7) that

$$r_n^{k+1} = \operatorname*{argmin}_{r_n \in \mathcal{F}_n} \left\| r_n - \left(r_n^k - \gamma \frac{\partial L}{\partial r_n} \right) \right\|_2^2$$

for $n \in \mathcal{N}$ and $k \ge 0$. Hence, Algorithm A1 is in fact a gradient projection method. Details on gradient projection methods can be found in [17, Chapter 3.3.2].

B. Asynchronous Decentralized Algorithm

The synchronous algorithm in section IV-A assumes that in each iteration, all EVs use the price profile in the last iteration to update their charging profiles, and the utility uses the new charging profiles to update the price. In reality, this synchronous computation may be impractical, especially when the number of EVs is large. In this section, we allow decisions to be made at different times with potentially outdated information. That is, in each iteration, only a subset of the EVs update their charging profiles, and the utility may or may not update the price. When an EV updates its charging profile, or the utility updates the price, they may use outdated information, i.e., information from the previous iterations.

We use an asynchronous model similar to that in [16], and allow EV $n \in \mathcal{N}$ to update at iterations $K_n \subseteq \{1, 2, \ldots\}$. At iterations $k \notin K_n$, we set $r_n^{k+1} = r_n^k$. Similarly let $K_u \subseteq \{1, 2, \ldots\}$ denote the set of iterations when the price is updated. At iterations $k \notin K_u$, we set $p^{k+1} = p^k$. At iterations $k \in K_n$, EV n updates its charging profile r_n^k according to (7), with p^k replaced by $p^{k-a_n(k)}$ due to delay $a_n(k)$. At iterations $k \in K_u$, the utility updates the price p^k according to (8), with r_n^k replaced by $r_n^{k-b_n(k)}$ due to delay $b_n(k)$. In general, we allow delays a_n and b_n to be k dependent but assume that they are uniformly bounded, i.e., $a_n(k) \leq d$, $b_n(k) \leq d$ for all n and all k. We also assume that each EV updates its charging profile at least once every d iterations, and the utility updates the price profile at least once every d iterations.

Algorithm A2: Given planning horizon $\mathcal{T}$, maximum number of iterations $K \in \mathbb{N}$, error tolerance $\epsilon > 0$, base load profile D, the number of EVs N, charging capacity R_n and charging rate upper bound $\overline{r}_n$ for EV $n \in \mathcal{N}$, pick a step size γ satisfying

$$0 < \gamma < \frac{1}{N\beta(3d+1)}.$$

1) Initialize the price profile and the charging profile as

$$p^0 := U'(D),\ r_n^0 := 0 \text{ for all } n.\ k \leftarrow 0.$$

2) If $k = 0$ or $k - 1 \in K_u$, the utility broadcasts the price profile p^k and the step size γ.
3) For each EV $n \in \mathcal{N}$, if $k \in K_n$, it calculates a new charging profile

$$r_n^{k+1} := \underset{r_n \in \mathcal{F}_n}{\operatorname{argmin}} \sum_{t \in \mathcal{T}} p^{k-a_n}(t) r_n(t) + \frac{1}{2\gamma}\left(r_n(t) - r_n^k(t)\right)^2,$$

and sends r_n^{k+1} to the utility.
4) If $k \in K_u$, the utility updates the price profile p^{k+1} as

$$p^{k+1} := U'\left(D + \sum_{n=1}^{N} r_n^{k+1-b_n}\right).$$

If $\left\|p^{k+1} - p^k\right\|_2 \leq \epsilon$, return p^{k+1}, r_n^{k+1} for all n.
5) If $k < K$, $k \leftarrow k + 1$, and go to step (2).
Else, return p^K, r_n^K for all n.

Similarly to the synchronous Algorithm A1 introduced in section IV-A, charging profile r^k of the asynchronous Algorithm A2 also converges to the set $\mathcal{O}$ as $k \to \infty$.

Theorem 5: If $\mathcal{F}$ is non-empty, then $r^k \to \mathcal{O}$ as $k \to \infty$. Let r^* be an optimal charging profile, then

- the aggregated charging profile converges to that of r^*, i.e.,
$$\lim_{k\to\infty} R^k = R_{r^*};$$
- the price profile converges to that corresponding to r^*, i.e.,
$$\lim_{k\to\infty} p^k = p(D + R_{r^*});$$
- the difference between two consecutive charging profiles of each EV converges to 0, i.e.,
$$\lim_{k\to\infty} \left\|r_n^{k+1} - r_n^k\right\|_2 = 0$$
for all $n \in \mathcal{N}$.

Proof: In the Appendix.

V. CASE STUDIES

In this section, we first evaluate the optimality of Algorithm A1 and then compare the convergence rates of Algorithm A1 (synchronous) and Algorithm A2 (asynchronous). We compare the optimality and convergence rate of Algorithm A1 with those of the decentralized scheduling algorithm proposed in [13], in *homogeneous* and *non-homogeneous* cases. By *homogeneous* we mean all EVs plug in at the same time with the same charging demand and maximum charging rate, and have a common deadline. By *non-homogeneous*, we mean EVs may plug in at different times with different charging demands and maximum charging rates (yet they are available for negotiation at the beginning of the planning horizon), and have different deadlines. For notational brevity, we call the algorithm in [13] DAP, standing for "Deviation from Average Penalty." Recall that the optimality of DAP is only guaranteed in the homogeneous case. We choose the average residential load profile in the service area of South California Edison from 20:00 on February 13th, 2011 to 19:00 on February 14th, 2011 as the normalized base demand profile per household. According to the typical charging characteristics of EVs in [14], we set $\overline{r}_n(t) = 3.3$ kW if EV n is plugged in at time t, and 0 kW otherwise. We assume that the charging rate $r_n(t)$ takes values in $[0, \overline{r}_n(t)]$ and consider the penetration level of $N = 1000$ EVs in 5000 households. The planning horizon is divided into 24 slots, each of an hour, during which the charging rate of each EV is not changed. The price function is taken to be $p(x) = x$. As used in [13], we choose the price function and parameters for Algorithm DAP as $p(x) = 0.15x^2$, $c = 1$, and $\delta = 0.15$.

Homogeneous: Figure 3 shows the normalized total demand profile in each iteration of Algorithm A1 and DAP in a homogeneous case. Both algorithms converge to a valley-filling charging profile. Moreover, Algorithm A1 converges with a single iteration, while DAP takes several iterations to converge. It can be easily shown that algorithm A1 will always converge after 1 iteration in homogeneous cases regardless of the choice of N, $\overline{r}_n$ and R_n.

Non-homogeneous capacities: Figure 4 shows the normalized total demand profiles at convergence of Algorithm A1 and DAP in a non-homogeneous case where EVs have different charging capacities R_n. Algorithm A1 still converges to a valley-filling charging profile in a few iterations while DAP no longer converges to a valley-filling charging profile. The optimality proof provided in [13] does not straightforwardly extend to non-homogeneous cases.

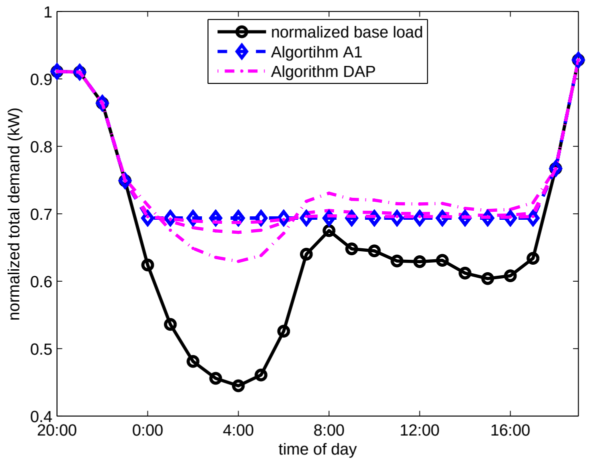

Fig. 3. Normalized total demand profiles in each iteration of Algorithm A1 and DAP in a homogeneous case. All EVs plug in at 20:00 with charging capacity $R_n = 10kWh$ and have a deadline at 19:00 on the next day. Multiple purple total demand profiles correspond to total demand profiles in different iterations of Algorithm DAP.

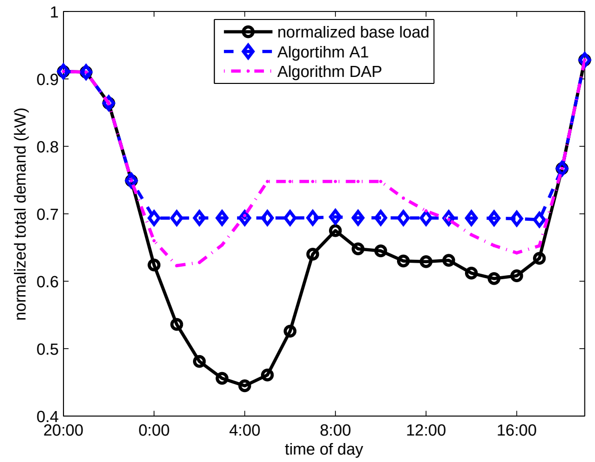

Fig. 5. Normalized total demand profiles at convergence of Algorithm A1 and DAP in a non-homogeneous case. EVs plug in uniformly between 20:00 and 5:00 with charging capacity $R_n = 10kWh$, and have deadlines uniformly distributed in [10:00,19:00] on the next day.

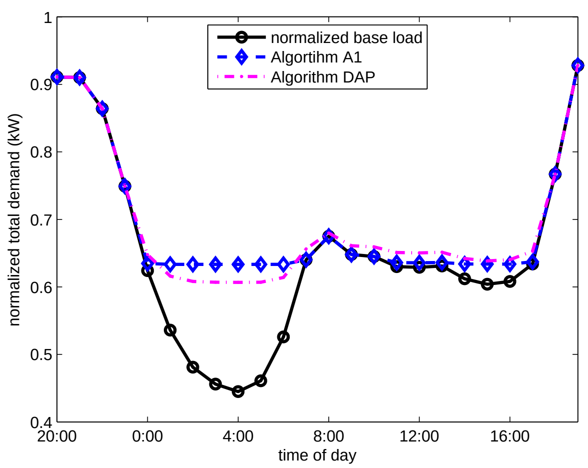

Fig. 4. Normalized total demand profiles at convergence of Algorithm A1 and DAP in a non-homogeneous case. All EVs plug in at 20:00 and have deadline 19:00 the next day, but with charging capacities R_n uniformly distributed in $[0, 10kWh]$.

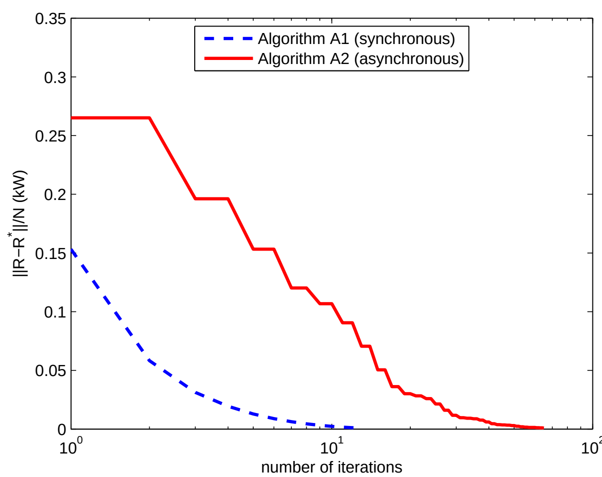

Fig. 6. The l_2 norm $\frac{1}{N}\|R^k - R^*\|$ of the normalized difference $\frac{1}{N}(R^k - R^*)$ between the aggregated charging profile R^k in iteration k in Algorithm A1 or A2 and the optimal aggregated charging profile. EVs plug in uniformly between 20:00 and 5:00 with charging capacity 10kWh, and have deadlines uniformly distributed in [10:00,19:00] on the next day. In the asynchronous setting, all EVs update their charging profiles and the utility updates price profile in iteration $k = 1, 3, 5, \ldots$, with outdated information $\hat{p}^{k-1} = p^{k-2}$ and $\hat{r}_n^k = r_n^{k-1}$.

Non-homogeneous plug-in times and deadlines: Figure 5 shows the normalized total demand profiles in another non-homogeneous case where EVs have the same charging capacity, but different plug-in times and deadlines. Algorithm A1 still converges to a valley-filling charging profile within few iterations, while Algorithm DAP yields a charging profile far from valley-filling. This is because Algorithm DAP uses a penalty term to limit the deviation of the EV charging profiles from the average charging profile. EVs have different charging horizons, but have to track the same average charging profile. At higher EV penetration levels, the difference becomes more significant. Algorithm A1 changes “deviation from the average penalty” to “deviation from the last iteration penalty.” While preserving its convergence property, Algorithm A1 no longer requires different EVs to track a common average charging profile. Hence, it successfully deals with the issue of heterogeneity in charging deadlines.

Comparison of convergence rates of synchronous and asynchronous algorithms: Figure 6 compares the convergence rates of Algorithm A1 and Algorithm A2. It can be seen that the asynchronous Algorithm A2 takes more iterations to converge, which is not surprising, since the information used by each EV is not necessarily updated in each iteration and outdated information may be used in some of the iterations. However, Algorithm A2 still converges with bounded delay and usage of outdated information, which makes it robust to communication delays and failures.

VI. Critique and Extensions

Objectives beyond flattening the aggregate demand: We focused on the objective of flattening the aggregate electricity demand. On the other hand, the algorithms proposed here can be extended to achieve other objectives including tracking an aggregate demand profile pre-specified by the utility in order to establish reserves and regulations against variations in generation (e.g., due to intermittent renewables) and demand (e.g., due to uncontrollable load variations). Moreover, the controllable load considered in the current paper is at the level of individual EVs. Extensions to a more realistic case where EV load aggregators (rather than individual EVs) participate negotiation are straightforward.

Offline v.s. online algorithms: The algorithms proposed in this paper are offline in the sense that all EVs are available for negotiation at the beginning of the planning horizon, and decisions are made with full information about each EV. A more realistic model, that we call online, would incorporate the EVs as they become available for negotiation, e.g., when they plug in for charging, over time and utilize predictions on future EV demand (rather than the exact values). Moreover, since the state of the system changes over time, the problem data would be updated over time. In such an online setting, even appropriate notions of "valley-filling" are subject to research. On the other hand, using the valley-filling notion of the current paper, our preliminary work has focused on modifications of Algorithm A1 in an online, shrinking-horizon setup (where EVs have common deadline, e.g., in the morning, but they may participate negotiation and plug in at different times). A preliminary result suggests that in the cases where valley-filling charging profiles exist and the predictions on the EV demand are accurate enough, then this shrinking-horizon algorithm yields a valley-filling profile. Our current work focuses on extending to a rolling horizon setup (where the EVs are not required to have common deadlines) and on quantifying the effects of prediction inaccuracies.

VII. Conclusions

In this paper, we studied utilizing decentralized EV charging control to fill the overnight electricity demand valley. We formulated it as an optimization problem, and showed that optimal charging profile minimizes the l_2 norm of the total demand. We proposed decentralized offline and online algorithms for solving the problem. In each iteration of these algorithms, each EV calculates its own charging profile according to the price profile broadcast by the utility, and the utility guides their behavior by updating the price profile. We proved that the offline algorithms converge to optimal charging profiles, and showed that online algorithms yield near optimal charging profiles, with only a scalar prediction of future EV charging demand. Simulation results are used to illustrate and validate these results.

Appendix

Lemma 3: Define $\pi_k := \sum_{n=1}^N \left\|r_n^{k+1} - r_n^k\right\|$. If $\mathcal{F}$ is non-empty and $\gamma < \frac{1}{N\beta(3d+1)}$, then $\pi_k \to 0$ as $k \to \infty$.

Proof: If $\mathcal{F}$ is non-empty, $\mathcal{F}_n$ is non-empty for all $n \in \mathcal{N}$. By repeating the proof in Lemma 1, we can show that

$$\left\langle p^{k-a_n}, r_n^{k+1} - r_n^k \right\rangle \le -\frac{1}{\gamma}\left\|r_n^{k+1} - r_n^k\right\|_2^2$$

for $n \in \mathcal{N}$ and $k \ge 1$. Hence,

$$\begin{aligned}
&\left\langle U'\left(D^{k+1}\right), r_n^{k+1} - r_n^k \right\rangle \\
&= \left\langle p^{k-a_n}, r_n^{k+1} - r_n^k \right\rangle + \left\langle U'\left(D^{k+1}\right) - p^{k-a_n}, r_n^{k+1} - r_n^k \right\rangle \\
&\le -\tfrac{1}{\gamma}\left\|r_n^{k+1} - r_n^k\right\|^2 + \left\|U'\left(D^{k+1}\right) - p^{k-a_n}\right\| \left\|r_n^{k+1} - r_n^k\right\|
\end{aligned}$$

for $n \in \mathcal{N}$ and $k \ge 1$. Choose $c \ge 0$ such that

$$k - a_n - c = \min\{l \le k - a_n \mid l - 1 \in K_u\}.$$

Then, $0 \le c \le d - 1$ and

$$\begin{aligned}
&\left\langle U'\left(D^{k+1}\right), r_n^{k+1} - r_n^k \right\rangle + \tfrac{1}{\gamma}\left\|r_n^{k+1} - r_n^k\right\|^2 \\
&\le \left\|r_n^{k+1} - r_n^k\right\| \left\|U'\left(D^{k+1}\right) - p^{k-a_n-c}\right\| \\
&= \left\|r_n^{k+1} - r_n^k\right\| \\
&\qquad \cdot \left\|U'\left(D^{k+1}\right) - U'\left(D + \textstyle\sum_{n=1}^N r_n^{k-a_n-c-b_n}\right)\right\| \\
&\le \beta\left\|r_n^{k+1} - r_n^k\right\| \left\|R^{k+1} - \textstyle\sum_{n=1}^N r_n^{k-a_n-c-b_n}\right\| \\
&\le \beta\left\|r_n^{k+1} - r_n^k\right\| \left(\textstyle\sum_{n=1}^N \left\|r_n^{k+1} - r_n^{k-a_n-c-b_n}\right\|\right) \\
&\le \beta\left\|r_n^{k+1} - r_n^k\right\| \left(\textstyle\sum_{n=1}^N \sum_{l=k-a_n-c-b_n}^k \left\|r_n^{l+1} - r_n^l\right\|\right) \\
&\le \beta\left\|r_n^{k+1} - r_n^k\right\| \left(\textstyle\sum_{n=1}^N \sum_{l=k-3d}^k \left\|r_n^{l+1} - r_n^l\right\|\right)
\end{aligned}$$

for $n \in \mathcal{N}$ and $k \ge 1$. Then,

$$\begin{aligned}
&\left\langle U'\left(D^{k+1}\right), R^{k+1} - R^k \right\rangle + \frac{1}{\gamma}\sum_{n=1}^N \left\|r_n^{k+1} - r_n^k\right\|^2 \\
\le\;& \beta \sum_{m=1}^N \left\|r_m^{k+1} - r_m^k\right\| \sum_{n=1}^N \sum_{l=k-3d}^k \left\|r_n^{l+1} - r_n^l\right\| \\
=\;& \beta\pi_k \sum_{l=k-3d}^k \pi_l \\
\le\;& \beta\left(\left(1 + \frac{3d}{2}\right)\pi_k^2 + \frac{1}{2}\sum_{l=k-3d}^{k-1} \pi_l^2\right)
\end{aligned}$$

for $k \ge 1$. Hence,

$$\begin{aligned}
&L(r^{k+1}) - L(r^k) \\
\le\;& \left\langle U'\left(D^{k+1}\right), R^{k+1} - R^k \right\rangle \\
\le\;& \beta\left(\left(1 + \frac{3d}{2}\right)\pi_k^2 + \frac{1}{2}\sum_{l=k-3d}^{k-1} \pi_l^2\right) \\
&\qquad - \frac{1}{\gamma}\sum_{n=1}^N \left\|r_n^{k+1} - r_n^k\right\|^2 \\
\le\;& \frac{\beta}{2}\sum_{l=k-3d}^{k-1} \pi_l^2 + \left(\beta\left(1 + \frac{3d}{2}\right) - \frac{1}{N\gamma}\right)\pi_k^2
\end{aligned}$$

for $k \geq 1$ and

$$\begin{aligned} & L(r^{k+1}) - L(r^1) \\ \leq \quad & \frac{3d}{2}\beta\sum_{l=0}^{k-1}\pi_l^2 + \left(\beta\left(1+\frac{3d}{2}\right) - \frac{1}{N\gamma}\right)\sum_{l=1}^{k}\pi_l^2 \\ \leq \quad & \left(\beta(3d+1) - \frac{1}{N\gamma}\right)\sum_{l=1}^{k}\pi_l^2 + \frac{3d}{2}\beta\pi_0^2. \end{aligned} \tag{14}$$

Since $\gamma < \frac{1}{N\beta(3d+1)}$,

$$\beta(3d+1) - \frac{1}{N\gamma} < 0. \tag{15}$$

If π_k does not converge to 0 as k tends to infinity, then $L(r^{k+1}) \to -\infty$ as $k \to \infty$. However, $L(r^{k+1})$ is bounded below by its definition. Hence, $\pi_k \to 0$ as $k \to \infty$. $\square$

As a consequence of Lemma 3,

$$\begin{aligned} & \left\|U'(D^{k+1}) - U'(D^k)\right\| \\ \leq \quad & \beta\|R^{k+1} - R^k\| \\ \leq \quad & \beta\pi_k \to 0 \text{ as } k \to \infty. \end{aligned}$$

Similarly, $\left\|p^k - U'(D^k)\right\| \to 0$ as $k \to \infty$. This implies that, after a number of iterations, real price profile $U'(D^k)$ and its delayed version p^k (used by EVs to update their charging profiles) become close, and we can expect that our algorithm converges to optimal charging profiles even with delay.

For a given charging profile r, define the distance to the set of optimal charging profiles as following

$$d(r, \mathcal{O}) := \inf_{r' \in \mathcal{O}} \|r - r'\|.$$

Lemma 4: For a sequence $\left\{r^k\right\}_{k\geq 1} \subseteq \mathcal{F}$ of feasible charging profiles, if $d(r^k, \mathcal{O})$ does not converge to 0 as $k \to \infty$, then there exist a positive constant $\delta > 0$ and a subsequence $\left\{r^{k_i}\right\}_{i\geq 1}$ such that

$$k_{i+1} - k_i \geq d, \tag{16}$$

$$d(r^{k_i}, \mathcal{O}) \geq \delta. \tag{17}$$

for $i \geq 1$.

Proof: If $d(r^k, \mathcal{O})$ does not converge to 0 as $k \to \infty$, then there exists $\delta > 0$, such that for any $K \in \mathbb{N}$, there exists $k > K$ with

$$d(r^k, \mathcal{O}) \geq \delta.$$

We construct the subsequence $\left\{r^{k_i}\right\}_{i\geq 1}$ as following:

- Let $K = 1$, choose $k_1 > K$ such that $d(r^{k_1}, \mathcal{O}) \geq \delta$.
- Suppose we already get $k_1, \ldots, k_m$ ($m \geq 1$), satisfying (16) for $i = 1, \ldots, m-1$ and (17) for $i = 1, \ldots, m$. Let $K = k_m + d$, choose $k_{m+1} > K$ such that $d(r^{k_{m+1}}, \mathcal{O}) \geq \delta$.

It is easy to check that the subsequence $\left\{r^{k_i}\right\}_{i\geq 1}$ satisfies (16) and (17) for $i \geq 1$ by induction. $\square$

Proof for Theorem 5: Denote r^k as the charging profile of all EVs in iteration k of Algorithm A2. We first prove that $r^k \to \mathcal{O}$ as $k \to \infty$ by contradiction. Assume that r^k does not converge to the set $\mathcal{O}$ as $k \to \infty$, then $d(r^k, \mathcal{O})$ does not converge to 0. By Lemma 4, we can find a subsequence $\left\{r^{k_i}\right\}_{i\geq 1}$ satisfying (16) and (17) for $i \geq 1$. Since $\mathcal{F}$ is compact, we can find a convergent subsequence $\{r^{k_{i_s}}\}_{s\geq 1}$ of $\left\{r^{k_i}\right\}_{i\geq 1}$ such that

$$r^{k_{i_s}} \to r^* = (r_1^*, \ldots, r_N^*) \text{ as } s \to \infty.$$

It's not difficult to show that $d(r^*, \mathcal{O}) \geq \delta$. For brevity, we use $\left\{r^{k_i}\right\}_{i\geq 1}$ to denote the sequence $\{r^{k_{i_s}}\}_{s\geq 1}$, then

$$r^{k_i} \to r^* = (r_1^*, \ldots, r_N^*) \text{ as } i \to \infty.$$

Lemma 3 implies that $\pi_k \to 0$ as $k \to \infty$. Hence, $r^{k_i+j} \to r^*$ as $i \to \infty$ for all $j \in \{0, \ldots, d-1\}$. Define

$$p^* := U'(D + R_{r^*}).$$

Since $r^* \notin \mathcal{O}$, r^* is not a stationary point for Algorithm A1 (Corollary 2). Hence, there exists n such that

$$r_n' := \operatorname*{argmin}_{r_n \in \mathcal{F}_n} \langle p^*, r_n\rangle + \frac{1}{2\gamma}\|r_n - r_n^*\|^2 \neq r_n^*.$$

EV n updates its charging profile r_n at least once during iterations $[k_i, k_i + d - 1]$ for $i \geq 1$. Assume that it updates at iteration $k_i + j_i$ where $j_i \in [0, d-1]$, then

$$\|r_n^{k_i+j_i+1} - r_n^{k_i+j_i}\| \to \|r_n' - r_n^*\| > 0 \text{ as } i \to \infty.$$

Hence, for i sufficiently large,

$$\sum_{l=k_i}^{k_i+d-1}\pi_l \geq \pi_{k_i+j_i} \geq \|r_n^{k_i+j_i+1} - r_n^{k_i+j_i}\| > \frac{1}{2}\|r_n' - r_n^*\| > 0$$

and

$$\sum_{l=k_i}^{k_i+d-1}\pi_l^2 \geq \frac{1}{d}\left(\sum_{l=k_i}^{k_i+d-1}\pi_l\right)^2 > \frac{1}{4d}\|r_n' - r_n^*\|^2 > 0.$$

It follows from (14) that $L(r^{k+1}) \to -\infty$ as $k \to \infty$. However, $L(r^{k+1})$ is bounded below by its definition, contradict. Hence, $r^k \to \mathcal{O}$ as $k \to \infty$. The rest of the proof follows along the lines of that for Theorem 4. $\square$

Acknowledgment

The authors express gratitude to K. Mani Chandy and Sachin Adlakha for inspiring discussions.

References

[1] "Environmental assessment of plug-in hybrid electric vehicles - volume 1: nationwide greenhouse gas Emissions," Electric Power Research Institute, 2007. Available: http://my.epri.com/portal/server.pt?

[2] Committee on assessment of resource needs for full cell and hydrogen technologies, National Research Council, *Transitions to alternative transportation technologies–plug-in hybrid electric vehicles*, the National Press, 2010.

[3] U.S. Department of Energy website http://www.eere.energy.gov/. Available: http://tinyurl.com/4o5ggml

[4] L. Kelly, A. Rowe and P. Wild, "Analyzing the impacts of plug-in electric vehicles on distribution networks in British Columbia," *in Proc. Electrical Power & Energy Conference*, 2009, pp. 1-6.

[5] C. Roe, F. Evangelos, J. Meisel, A. P. Meliopoulos and T. Overbye, "Power system level impacts of PHEVs," *in Proc. Hawaii International Conference on System Science*, 2009, pp. 1-10.

[6] K. Clement, E. Haesen and J. Driesen, "Coordinated charging of multiple plug-in hybrid electric vehicles in residential distribution grids," *in Proc. Power Systems Conference and Exposition*, 2009, pp. 1-7.

[7] J. A. P. Lopes, F. J. Soares and P. M. R. Almeida, "Integration of electric vehicles in the clectric power system," *Proceedings of the IEEE*, vol. 99, No. 1, 2011, pp. 168-183.

[8] C. Quinn, D. Zimmerle and T. H. Bradley, "The effect of communication architecture on the availability, reliability, and economics of plug-in hybrid electric vehicle-to-grid ancillary services," *Journal of Power Sources*, vol. 195, issue 5, 2010, pp. 1500-1509.

[9] J. A. P. Lopes, P. M. R. Almeida, and A. M. M. da Silva, "Smart charging strategies for electric vehicles: Enhancing grid performance and maximizing the use of variable renewable energy sources," *in Proc. International Battery, Hybrid and Fuel Cell Electric Vehicle Symposium and Exhibition*, 2009, pp. 1-11.

[10] S. Shao, T. Zhang, M. Pipattanasomporn and S. Rahman, "Impact of TOU rates on distribution load shapes in a smart grid with PHEV penetration," *in Proc. Transmission and Distribution Conference and Exposition*, 2010, pp. 1-6.

[11] E. Sortomme, M. M. Hindi, S. D. J. MacPherson and S. S. Venkata, "Coordinated charging of plug-in hybrid electric vehicles to minimize distribution system losses," *IEEE Transactions on Smart Grid*, vol. 2, no. 1, 2011, pp. 198-205.

[12] M. C. Caramanis and J. M. Foster, "Coupling of day ahead and real-time power markets for energy and reserves incorporating local distribution network costs and congestion," *in Proc. Allerton Conference on Communication, Control, and Computing*, 2010, pp. 42-49.

[13] Z. Ma, D. Callaway and I. Hiskens, "Decentralized charging control for large populations of plug-in vehicles," *in Proc. Conference on Decision and Control*, 2010, pp. 206-212.

[14] A. Ipakchi and F. Albuyeh, "Grid of the future," *IEEE Power and Energy Magazine*, vol. 7, no. 2, 2009, pp. 52-62.

[15] South California Edison website http://www.sce.com/. Available: http://www.sce.com/005_regul_info/eca/DOMSM11.DLP

[16] S. H. Low and D. E. Lapsley, "Optimization flow control, I: Basic algorithm and convergence," *IEEE/ACM Transactions on Networking*, 1999, pp. 861-874.

[17] D. P. Bertsekas and J. N. Tsitsiklis, "Parallel and Distributed Computation," Prentice-Hall, 1989.

[18] S. Boyd and L. Vandenberghe, "Convex Optimization," Cambridge University Press, 2004.